MOGAS M7
A PERFORMANCE ENHANCED NANO STRUCTURED TITANIUM DIOXIDE COATING IN HPAL AND POx BALL VALVE APPLICATIONS

By

[1]George (Yunfei) Qiao, [1]Jonquil Hill, [2]Sunil Musali

[1]MOGAS Industries, Houston, Texas, USA
[2]F.W. Gartner, Houston Texas, USA

Presenter and Corresponding Author

George (Yunfei) Qiao, Ph.D.
gqiao@mogas.com

ABSTRACT

Current industry coating specifications often include stringent chemical (composition and stoichiometry) and physical (hardness, porosity, thickness, structure, bond strength, interfacial contamination, etc.) requirements due to the severity of operating conditions. However, several additional control variables inherent to the coating application and manufacturing process, if overlooked, can result in properties that result in reduced equipment service life and inadequate field performance.

MOGAS Industries, in conjunction with our coating partner, have spent considerable time and resources researching and developing additional processing and test protocols for our patented n-TiO_2 coatings, to ensure advancements in performance and reliability for field applications. This publication will detail some of the test methods and quality controls used in further enhancing the overall performance of our M7 nanostructured Titanium Dioxide (n-TiO_2) coating. We will also present the enhancement of some of the key properties of M7 Titanium Dioxide to compare it with other commercially available ceramic coatings, including the widely accepted chromium oxide coatings, and look at the differences in their field performance.

Severe service metal-seated ball valves' ability to operate and isolate in extreme environments with corrosive and abrasive solids has made them the preferred product for isolating and directing the flow of hot slurry within HPAL (i.e., Ni/Co) and POx (i.e., Au and Cu) autoclave systems. To withstand the harsh environment of these autoclaves, these ball valves incorporate protective thermal sprayed coatings to minimize wear and corrosion, thereby maximizing valve sealing life in these severe applications.

As a result of our tenure in this industry, MOGAS understands that the performance of any metal-seated ball valve is highly dependent on the quality, consistency and property enhancement of any applied protective coating. MOGAS Industries' patented nanostructured Titanium Dioxide (n-TiO_2) coating has shown superior corrosion and abrasion resistance for over a decade. Because of the proven ability of our products and coatings to meet the Industry demands for improved efficiency, reduced operating cost and longer life for critical equipment, MOGAS has been a dominant critical valve provider in the autoclave industry.

INTRODUCTION

HPAL and POx technologies make use of extreme processing environments to economically leach and extract nickel, cobalt and gold from low-grade ore. The current HPAL processing environment consists of high temperature (> 250 ºC/ 480 °F) corrosive (up to 98 % sulfuric acid) slurry (20 wt% solids) at high pressures (up to 798 psi/ 5.5 MPa). The POx environment also consists of hot (115 – 225 ºC/ 239 –437 °F) sulfuric acid solutions (10 – 15 g/L free acid) with high solids (12 to 50 wt%) content and high oxygen partial (up to 400 psi/ 2.75 MPa) and operating (up to 470psi/ 3.25 MPa) pressures.

Metal-seated ball valves' ability to operate in severe service autoclave environments with crushed, abrasive solids is largely dependent on proper substrate material selection and incorporation of one or more protective thermal sprayed coating(s).

However, anomalies in thermal spray coatings are inherent to the coating application process and may provide a path for sulfide and chloride attacks or crack initiation, which would impact the field performance of a metal-seated ball valve. Several failure mechanisms in various valve applications involving different base metals are discussed below.

Sulfide Attack

Sulfide formation was identified by EDS (Electron Dispersive Spectroscopy) at the interface of a ceramic coating and Super Duplex stainless steel base metal as shown in Figures 1a and 1b. Figure 1a shows the cross section of coating/ base metal that was scanned, the high sulfur concentrations at depths of 10 - 22µm show permeation of sulfur to the base metal. The presence of corrosive products at the base metal will cause coating delamination.

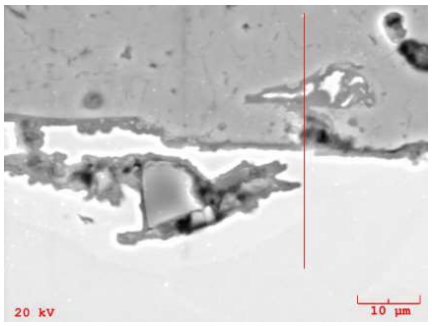

Figure 1a: TiO_2 coating on F53 base metal

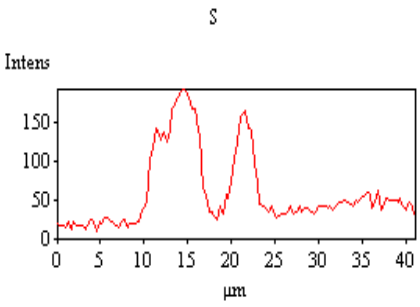

Figure 1b: EDS sulfur profile across the top coating, interface and base metal.

Chloride and Sulfide Attack

Figures 2a and 2b show that both chloride and sulfide corrosion products were identified by Auger spectroscopy on a corroded 6" (150mm) 600# Superaustenitic stainless steel ball in Oxygen/Steam Service.
Auger Spectroscopy analysis is used to detect the presence of elements in minute quantities (≥ 100 ppm levels) with small error margins, EDS analysis detects element concentrations in the range of about 0.1 to 0.3% with higher error margins.

Figure 2a shows micro pitting on the Alloy 20 base metal, caused by the presence of both sulfides and chlorides.

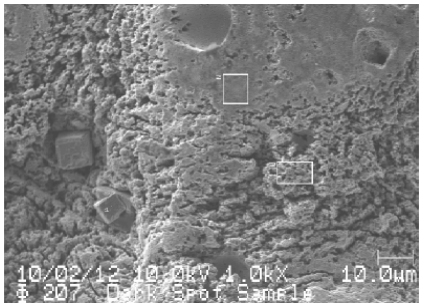

Figure 2a: Severely corroded Alloy 20.

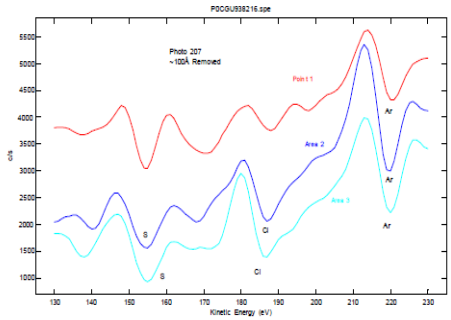

Figure 2b: Cl, S signature identified by Auger.

Thermally Induced Cracking

Thermally induced cracking is another in service phenomenon of concern on Superaustenitic/ Ceramic coating combinations due to the high mismatch of Expansion Coefficients between ceramic coatings and austenitic base metals. Figure 3 shows thermally induced cracks on a n-TiO_2/Alloy 20 coupon after heating to 600 °C (1,112 °F) and rapid quenching in cold water. This test was performed at temperatures way out of the range of normal autoclave operating temperatures, however, no corrosive or abrasive media were present. When tested at elevated temperatures (600 °C/ 1,112 °F) cracking was observed after 10 thermal cycles, when repeated at actual operating temperatures (230 ºC/ 450 ºF), no thermal cracking occurred.

Figure 3: Thermally induced cracks on a n-TiO_2/Alloy 20 coupon.

Even though some coating anomalies cannot be totally eliminated, they can be minimized through feedstock control, proper equipment maintenance and well trained operators. Selection of proper coating structure to match the properties of the base metal is critical for maximizing valve sealing life in severe service applications. In addition, it is imperative that proper quality controls and production testing are present to detect coating features/ properties that can negatively impact field performance.

The following presents MOGAS' approach through laboratory tests and field performance support to ensure superior coating performance in the severe HPAL and POx autoclave environment.

EXPERIMENTAL

To ensure that our patented nanostructured Titanium Dioxide coating is continually enhanced, MOGAS and our coating partner have been developing optimized application and process parameters and additional production testing methods to improve the performance and life of our coatings. Testing includes, but is not limited to, bend and low-load impact tests to evaluate physical characteristics as well as electrochemical analysis of coating/ base metal combinations to evaluate corrosion resistance.

Using different application and processing parameters, coatings were sprayed on Titanium Gr.5, Super Duplex and Superaustenitic stainless steel substrates to a thickness between 0.011" (279 µm) and 0.012" (305 µm).

Porosity

The porosity of a coating impacts its strength and adhesion to the base metal, a high level of porosity also allows the corrosive media to permeate through the coating at a faster rate than a denser coating with a lower porosity. During testing all porosity was measured following ASTM E2109-01 standard. Three measurements were taken for each sample at a magnification of 200X. Image analysis software was used to measure porosity levels; it can differentiate porosity from un-melted feedstock materials and coating splats.

Bond Strength

Bond strength is a measure of how well the coating adheres to the substrate; low bond strength can lead to premature failure by several mechanisms (shear, spallation). Coating Bond strength was measured using ASTM D4541-09 and an epoxy adhesive with a test strength of up to 12,500 psi (86 MPa). Three measurements were taken for each sample.

Microhardness

The wear resistance of a coating is directly related to its hardness. Microhardness was measured using ASTM E384-09. This involves a series of Vickers indentation tests using a 300g impact load. Eight measurements were taken for each sample.

Abrasion Test

This measures a coatings resistance to abrasive wear. A three-body abrasion test was carried out on all test samples according to ASTM G65 procedure B using a Dry Sand/Rubber Wheel apparatus and an applied load of 30lb (130N). The density used to convert mass loss to volume loss was measured from each coating sample. One sample was tested per coating type, with weight loss measured after every 300 revolutions.

Bend Test

Bend tests are often conducted on thermal spray coatings[1-6] to gauge the quality of the coating, which in turn is dependent on the working condition of the spray system and the quality of spray parameters used to apply the coating. The test consists of bending the coated samples around a 1" (25mm) diameter rod at 180 degrees (uncoated side in contact with the rod surface). Generally a "pass/fail" criterion is used. A coating sample is deemed to fail, if there are signs of coating lifting/spalling from the substrate when viewed by unaided eyes.

In this study, three to five samples, per coating type, were bend tested and averaged. Instead of a "pass/fail" rating, a quantitative rating system between 1 and 4 was developed(1 being the best and 4 being the worst). The ratings were assigned based on the resistance to damage of the coating in the vicinity of the bend. Quantitative analysis of coating loss for each sample, using an image analysis software, was performed to provide an objective rating for bend test resistance.

Low-load Impact Tests

Impact testing has been used extensively to gauge the quality of mostly metal or metal-base thermal spray coatings destined for different applications, i.e., boiler, hookpoints, spent nuclear fuel storage, electrical insulator, landing gear[1]. Different impact test systems are used, including: variations of hammer impact, ball impact, and gravelometry[1-4]. The objective is to select an impact testing system and appropriate test conditions that would instill visible damage to the coating after numerous impact cycles. Current industry testing practices use high impact loads which tend to fracture ceramic coatings on impact and prevent comparative toughness measurements being made between different coating systems. The n-TiO_2 coating, with its superior toughness over conventional ceramic coatings, will survive an adequate number of low-load impact cycles to warrant the use of impact testing in gauging its resistance to crack propagation and its bond strength.

The low-load impact test used in this study was carried out using the setup shown in Figure 4. A 2" (50mm) diameter steel ball was dropped from a consistent height onto a 1" x 3" x 0.25" (25mm x 75mm x 6mm) coated sample. The sample was fixed to ensure a single impact per drop. The number of impacts causing noticeable coating damage was recorded. Three samples per coating type were tested to determine an average value.

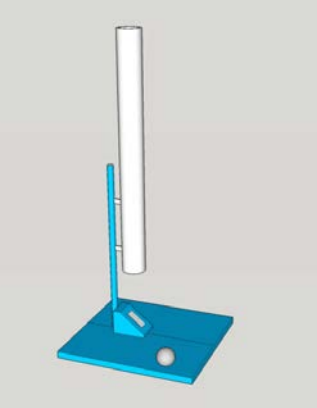

Figure 4: Low-load impact fixture.

Electrochemical Evaluations

Open circuit potential (OCP) and polarization tests were carried out at 50 ºC (122 °F) in 50:1 ratio of 5.1 Mol H_2SO_4 (acid) and NaCl (salt) solution.

Deleted:

OCP Testing measures coating/ substrate stability. Testing was performed for 48 hours in above solution.

Polarization tests were performed using the following test parameters:

Sample/working electrode exposure size: ~ (0.125 – 0.155 in^2/ 0.8– 1 cm^2)
Reference electrode: Saturated Calomel Electrode
Counter/auxiliary electrode: Platinum
Scan rate: 0.5 mV/s

During Polarization tests 0.5mV/s potential scan is applied across the test coupon in solution and the resultant current on the coating/ substrate is recorded which can be used to calculate corrosion rates. Two characteristics of a coating system can be determined from these tests, corrosion potential (E_{corr}) (how likely corrosion is to occur) and corrosion current density (i_{corr}) (if corrosion is going to occur, how fast will it progress).

These initial electrochemical tests were performed to measure the impact of varying coating process parameters on the corrosion rates of several coating systems, with the aim of selecting the best performers for further high pressure/ temperature autoclave testing using actual slurry solution. We will only present results for the autoclave tests on titanium substrates. Autoclave testing on Super Duplex and superaustenitic stainless steels is currently still in progress at the time of this publication.

RESULTS AND DISCUSSION

With the goal of optimizing our nanostructured Titanium Dioxide coating, MOGAS Industries and our coating partner embarked on an extensive research and development project to investigate the impact of varying spray application methods and process parameters on the characteristics and field performance of our coating. Our extensive experience in the autoclave industry has shown us that current specifications for ceramic coatings in these applications do not necessarily guarantee optimum performance in service. As a result of more than 10 years of field data and failure analysis, it was apparent that there were several other factors that are important to understand and measure in addition to the usual properties specified (porosity, bond strength, hardness etc.). Spray equipment, process parameters and variations to heat input at critical points all have a significant impact on the structure (and therefore performance characteristics) of the coating. The goal of this development is to develop an optimized M7 version of our n-TiO_2 coating by varying a multitude of parameters and measuring the results in a manner that can quantify actual field performance improvements.

At this stage five different spray application processes have been tested and the best process has been identified; in addition, the optimization of temperatures for different base metals and varied spray inputs has been completed to improve coating strength, ambient wear and corrosion resistance. The results presented on MOGAS n-TiO_2 coating samples have ALL passed typical coating specifications used to date by most ball valve OEMs for components destined for HPAL and POx applications (e.g. Microhardness > 700 $HV_{0.3}$/ Porosity ≤ 1.5 % / Bond Strength ≥ 10,000 psi/ 69 Mpa). In addition, we will demonstrate the advantages of our patented nanostructured Titanium Dioxide coating and compare key performance benefits of this coating with other commercially available ceramic coatings.

The n-TiO_2 coating samples (X1, Y1, M7-1) sprayed on Titanium Gr.5 substrates and (X2, Y2, M7-2) on Fe255 substrates presented in this publication were processed to meet current industry acceptance standards but were also further optimized, to improve performance.

Physical Characteristics

Figure 5 shows the cross-sectional micrographs of the coating samples. All coatings were dense with uniform thickness. The coating/substrate interfaces show no interface contamination from embedded grit used for surface profiling.

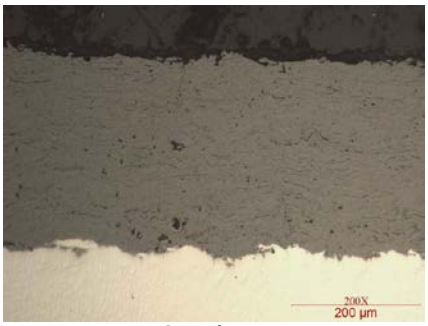

Sample X1

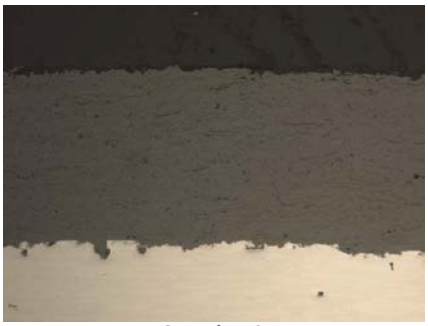

Sample X2

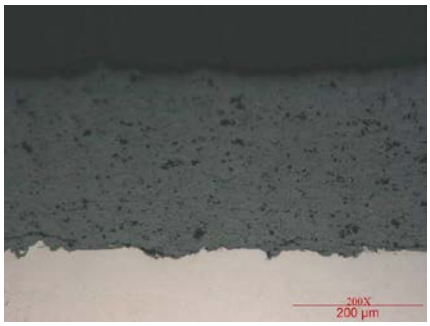

Sample Y1

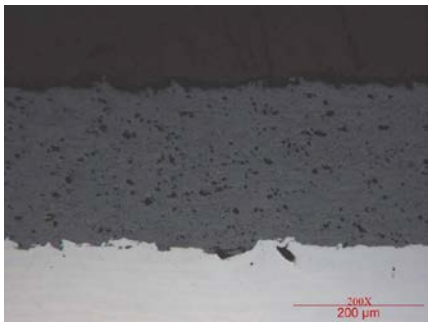

Sample Y2

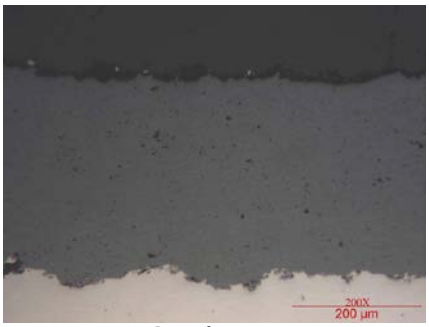

Sample M7-1

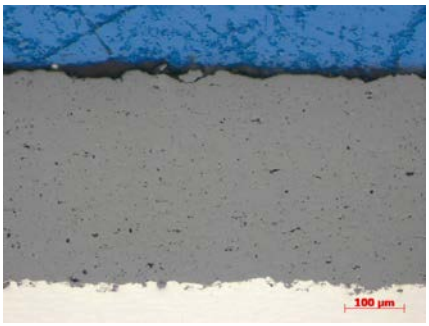

Sample M7-2

Figure 5: Cross-sectional micrographs of coating samples X1 (left top), Y1 (left middle) and M7-1 (left bottom) on TiGr.5 substrate, X2 (right top), Y2 (right middle) and M7-2 (right bottom) on Fe255 substrate.

Photographs of the n-TiO_2 coating samples after bend test and an example of image analysis of a bend tested samples are presented in Figures 6a and 6b.

As commonly observed in monolithic ceramic coatings, spallation of the coatings from the substrate is observed at the edges of the samples during bend testing. Transverse cracks are also observed along the radii of the bend regions. Samples M7-1 and M7-2 and Y1 and Y2 following the bend test had the lowest level of spallation and cracking; thus, showing superior strain tolerance compared to samples X1 and X2. There was a correlation between the resistance to bending strain and the level of measured porosity. This may reflect the fact that the presence of pores can lead to greater thermal and/or mechanical strain tolerance.

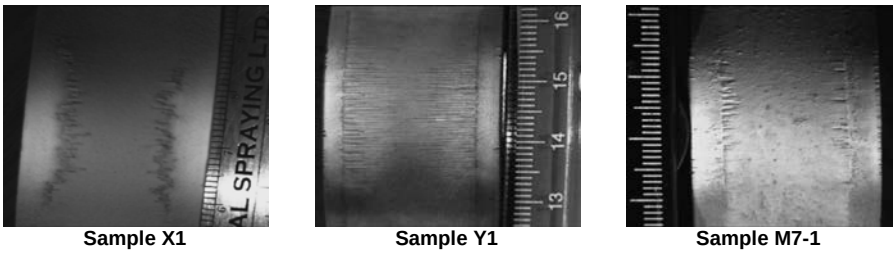

Sample X1 **Sample Y1** **Sample M7-1**

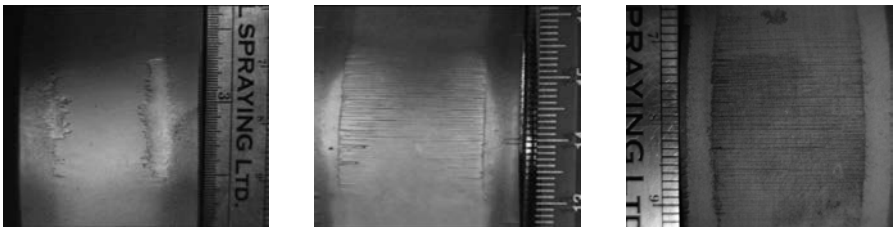

Sample X2 **Sample Y2** **Sample M7-2**

Figure 6a: Photographs of n-TiO_2 coating samples following bend testing – X1 (upper left), Y1 (upper center) & M7-1 (upper right) on TiGr.5 and X2 (lower left), Y2 (lower center) & M7-2 (lower right) on Fe255.

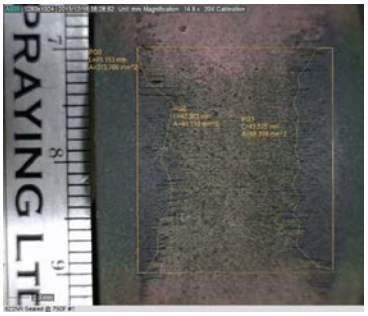

Figure 6b: Photograph of a bend tested sample with 31% coating loss.

The photograph in Figure 7 was taken after low-load impact testing and shows the onset of coating damage after a number of impacts.

Figure 7: Photograph of a n-TiO_2 coating sample following impact test.

The photograph in Figure 8 shows a typical test coupon after abrasion testing.

Three-body abrasion resistance has been incorporated by many of the ball valve OEMs to gauge and compare the wear resistance of coatings. Unfortunately, there is no common test method (or procedure) using standardized test loads with a rotating abrasive disc that forces manufacturers to report coating loss in a manner that allows the end user to compare them directly with one another. MOGAS has adopted the use of ASTM G65 procedure B using the actual coating density measured from each sample, as opposed to the theoretical density of the coating material.

Figure 8: Photograph of a n-TiO_2 coating sample following abrasion test.

The results of the physical characteristics and response to tests are presented in Table 1. Each coating was applied with different feedstock forms and process parameters optimized for each type. All six coating variations of the n-TiO_2 coating met the general specifications for HPAL and POx ball valves. Note: a few points regarding the data presented, firstly, the method of application and feedstock form have a significant impact on the properties of the coating, and secondly, within these samples, there seems to be a correlation between the hardness of the coating and both the abrasion and impact resistance. The former is commonly observed; however, the latter is not so obvious. In fact, harder materials are often found to be more brittle and thus one would expect them to be less resistant to impact, especially at 90° impingement angles. The higher impact resistance observed in samples M7 and Y may be attributed to the higher strain tolerance of nanostructured Titanium Dioxide coatings. As mentioned in previous publications relating to thermal sprayed nanostructured n-TiO_2 coatings[6-8], it is the combination of higher hardness and ductility that contribute to increased abrasive wear resistance. The same combination is favorable for impact resistance or toughness[9]. It is important to note that it is precisely the ability to gain ductility without compromising on hardness that sets nanostructured monolithic ceramic coatings apart with respect to superior wear performance compared to conventional coatings of the same composition.

Table 1: Physical Characteristics and Response to Tests

Sample	Porosity (%)	Bond Strength (psi)	Microhardness ($HV_{0.3}$)	Abrasion Volume Loss (mm^3)	Relative Bend Resistance*	Impact to Visible Damage
X1	0.15	11,361	858	33.13	4	30
Y1	0.65	11,070	931	23.76	1	70
M7-1	0.20	10,153	979	15.00	1	75
X2	0.20	> 12,500	884	32.34	3	21
Y2	0.75	> 12,500	935	23.95	1	37
M7-2	0.45	> 12,500	958	17.25	1	58

*Bend Test ranking: 1- less than 7.5% coating loss, 2- between 7.5% and 15% coating loss, 3- between 15% and 30% coating loss, 4- between 30% and 60% coating loss, Fail – above 60% coating loss.

Electrochemical Characteristics

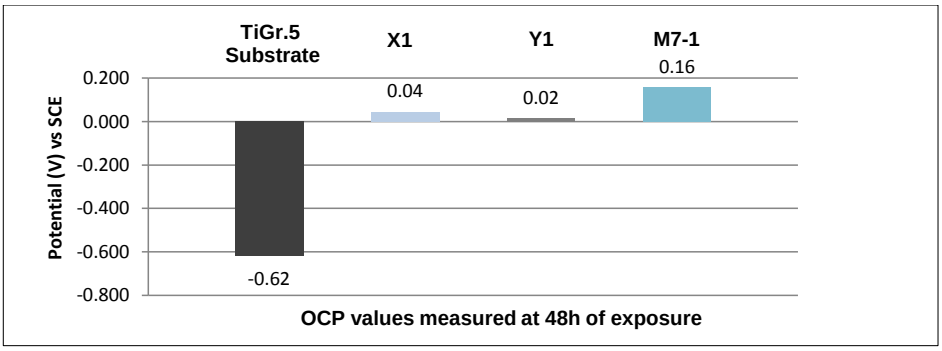

Figure 9a: Open circuit potential for samples X1, Y1, M7-1 and Titanium Gr.5 tested in a 50:1 solution of H_2SO_4 (acid) and NaCl (salt).

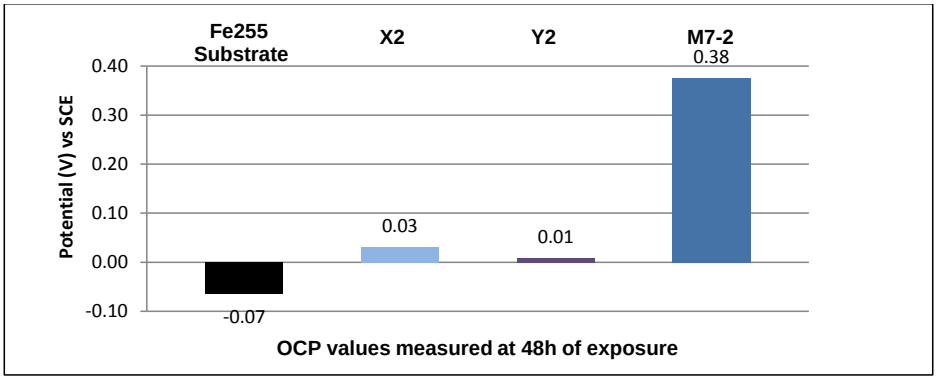

Figure 9b: Open circuit potential for samples X2, Y2, M7-2 and Fe255 tested in a 50:1 solution of H_2SO_4 (acid) and NaCl (salt).

Figure 9a and 9b show the OCP values of the n-TiO_2 coated samples along with the bare Titanium Gr.5 & Fe255 substrates in H_2SO_4/ NaCl solution. All coated samples exhibit a more positive OCP or stability in solution than the bare metal samples tested. Sample M7 (even on different base metals) had the

highest OCP followed by samples X, Y and bare Titanium Gr.5 & Fe255. This shows that the n-TiO2 coating has a higher corrosion resistance than the bare Titanium Gr.5 & Fe255.

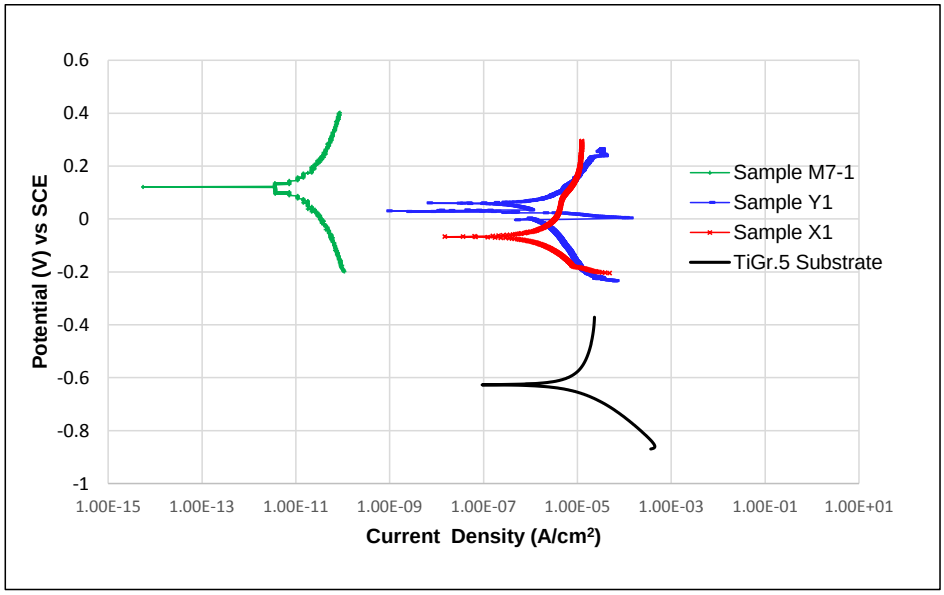

Figure 10a: Polarization curves for samples X1, Y1, M7-1 and Titanium Gr.5 substrate tested in a 50:1 solution of H_2SO_4 (acid) and NaCl (salt).

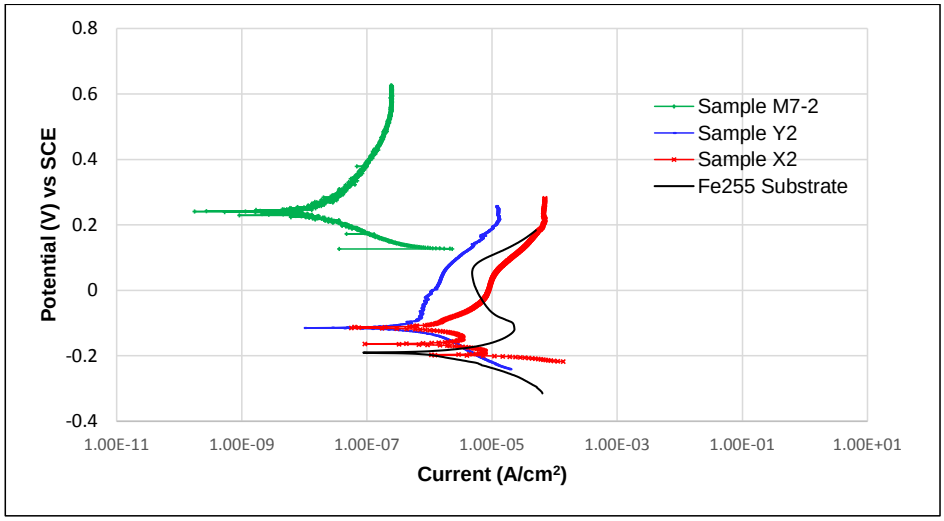

Figure 10b: Polarization curves for samples X2, Y2, M7-2 and Fe255 substrate tested a 50:1 solution of H_2SO_4 (acid) and NaCl (salt).

Table 2a: Measured Values of OCP, E_{corr} and i_{corr} of Titanium Gr.5 and n-TiO_2 Coated Titanium Gr.5 Samples

	TiGr.5 substrate	Sample X1	Sample Y1	Sample M7-1
OCP (V)	- 0.62	0.04	0.02	0.16
E_{corr} (mV)	- 626.56	- 67.17	48.41	106.83
i_{corr} ($\mu A/cm^2$)	17.97	7.48	0.91	3.87×10^{-6}

Table 2b: Measured Values of OCP, E_{corr} and i_{corr} of Fe255 and n-TiO_2 Coated Fe255 Samples

	Fe255 substrate	Sample X2	Sample Y2	Sample M7-2
OCP (V)	- 0.07	0.03	0.01	0.38
E_{corr} (mV)	- 190.59	- 113.75	-114.16	239.75
i_{corr} ($\mu A/cm^2$)	2.34	1.34	0.43	2.66×10^{-2}

Although the coating and substrate materials were the same for each group, there was significant difference in the corrosion properties between the samples. All coated samples of each base metal group exhibited higher E_{corr} and lower i_{corr} values compared to bare Titanium Gr.5 and Fe255 substrates.

As with the OCP results, the higher E_{corr} is a reflection of the barrier role the n-TiO_2 coating plays in mitigating attack of the electrolyte to the underlying Titanium Gr.5 and Fe255 substrates. The bare Titanium Gr.5 and Fe255 substrates showed a greater vulnerability to attack by the electrolyte. The most favorable results were observed in samples M7 with the highest E_{corr} and lowest i_{corr}. The corrosion rate, e.g., i_{corr}, does not correlate with the porosity levels observed for the samples; however, this may be due to the presence of other pathways (e.g., microcracks, gaps between splats) in the coating for the electrolyte to permeate to the substrate that was not identified within the scope of this work.

MOGAS M7 Performance vs. Other Commercial Coatings on Industry Accepted Alloys

MOGAS M7 coating was applied on F53 and Alloy 20 substrates and their bend, impact and corrosion resistance was compared with commercial Cr_2O_3 coatings (with a tantalum bond layer) on both F53 and Alloy 20 substrates.

The properties of M7 and other commercially available Cr_2O_3 coatings are presented in Table 3. It is important to note that the superior properties of M7 observed on Fe255 and Titanium Gr.5 substrates as shown in Table 1 are also evident on F53 and Alloy 20 substrates with the exception of low-load impact resistance (measure of coating toughness). A significant substrate effect found for F53/ M7 coating would outperform Alloy 20/ M7 under repeated low-load impact conditions. The lower impact resistance for M7 coated Alloy 20 is most likely due to the higher coefficients of thermal expansion (CTE) mismatch between the n-TiO_2 coating and Alloy 20, resulting in an inherently more brittle coating.

It is also important to note that the tantalum bond layer makes no significant contribution to the impact resistance for commercial Cr_2O_3 coating on both F53 and Alloy 20 substrates. However, without the tantalum bond layer, the commercial Cr_2O_3 coatings will fail bend tests as shown in Figure 11. This is due to the fact that the Cr_2O_3 coating has very little tolerance for mechanical strain (especially tensile strain). Without a bond layer, Cr_2O_3 will be more prone to CTE issues and subject to failure at a faster rate than n-TiO_2 coatings.

It can also be noted that higher hardness coatings will not necessarily outperform lower hardness alternatives; they may in theory have better wear resistance potential but they are more brittle and less resistant to strain and spallation.

Table 3: M7 and Commercial Cr_2O_3 Coating with a Tantalum Bond Layer on F53 and Alloy 20 Base Material

Sample	Porosity (%)	Bond Strength (psi)	Microhardness (HV0.3)	Relative Bend Resistance	Impact to Visible Damage
M7/F53	0.20	> 12,500	884	1	> 70
M7/Alloy 20	0.40	> 12,500	843	1	24.3
Cr_2O_3/Bond/F53	1.75	7,774	1098	3	50
Cr_2O_3/Bond/Alloy20	1.75	9,747	1147	3	57.3

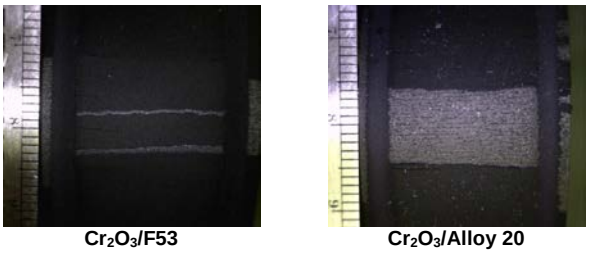

Cr_2O_3/F53 **Cr_2O_3/Alloy 20**

Figure 11: Photographs of Cr_2O_3 coating samples on F53 and Alloy 20 substrate following bend testing – Cr_2O_3/F53 (left), Cr_2O_3/Alloy 20 (right).

Figure 12 shows the OCP values of M7 and commercial Cr_2O_3 with a tantalum bond layer on F53 and Alloy 20 and the bare substrates in a 50:1 solution of H_2SO_4 (acid) and NaCl (salt). Although all coated samples exhibited a more positive OCP compared to the uncoated base metals, there are significant benefits for using M7 rather than Cr_2O_3 (with tantalum bond layer) on both F53 and Alloy 20 substrates. The significant substrate effect observed in the impact tests is also observed in the OCP results and stabilities for M7 on F53 and Alloy 20 substrates. This effect is evident in service when chlorides are present. MOGAS noted the impact that chloride presence had on lowering corrosion resistance of superaustenitic base metals; these chlorides were introduced into the autoclave during the brick cure process.

The electrochemical characteristics shown in Figure 13 and Table 4 further confirm the benefits of using M7 on F53 substrates rather than on Alloy 20. The superior performance of M7 on both substrates is also clearly seen over the commercial Cr_2O_3 coating (with a tantalum bond layer) since the M7 coatings exhibit higher E_{corr} (corrosion barrier) and lower i_{corr} (rate of corrosion) values than the Cr_2O_3 coatings.

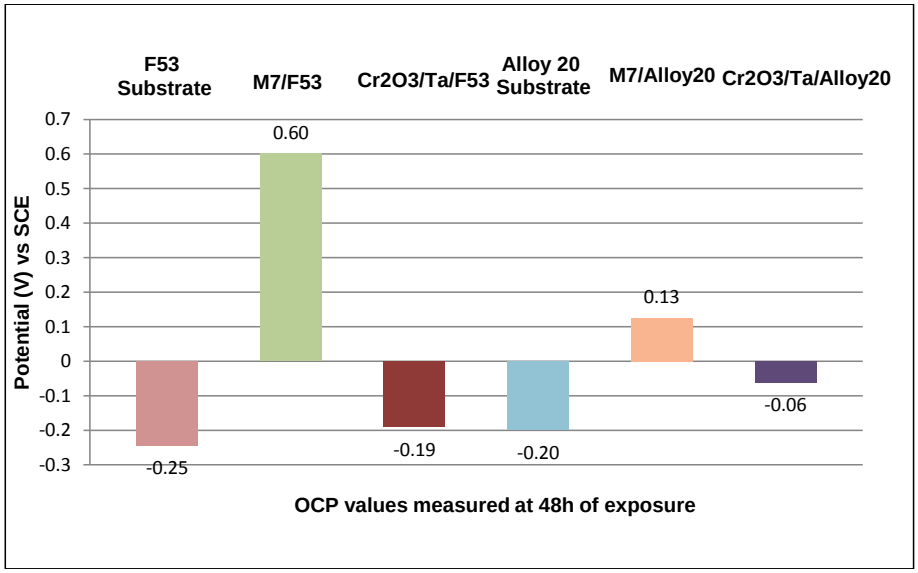

Figure 12: Open circuit potential for samples M7/F53, M7/Alloy20, Cr_2O_3/Ta/F53, Cr_2O_3/Ta/Alloy 20 and bare F53 and Alloy 20 substrates tested in a 50:1 solution of H_2SO_4 (acid) and NaCl (salt).

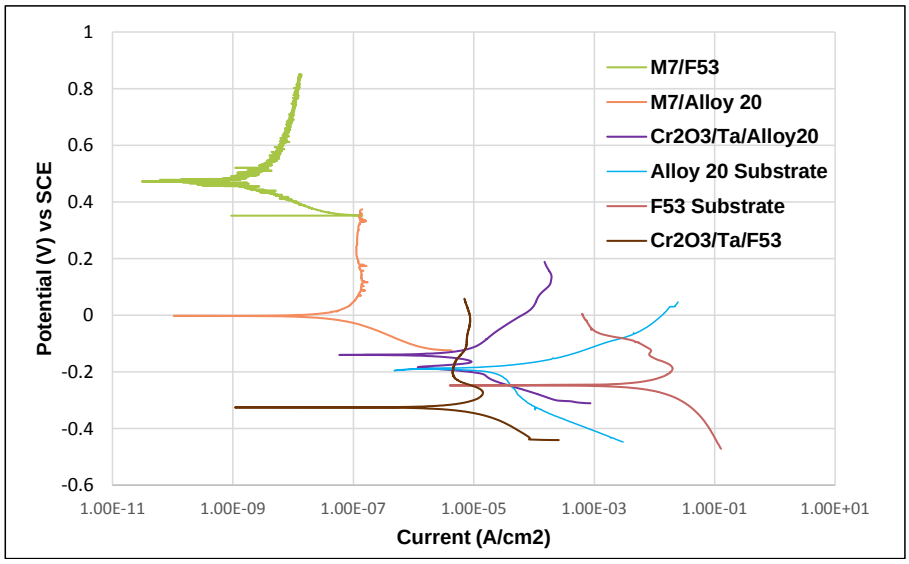

Figure 13: Polarization curves for Sample M7/F53, M7/Alloy 20, Cr_2O_3/Ta/F53, Cr_2O_3/Ta/Alloy 20 and bare F53 and Alloy 20 substrates tested in a 50:1 solution of H_2SO_4 (acid) and NaCl (salt).

Table 4: Measured Values of OCP, E_{corr} and i_{corr} of F53, Alloy 20, and M7 and Cr_2O_3/Ta Coated F53 and Alloy 20

	F53 substrate	M7/F53	Cr_2O_3/Ta/ F53	Alloy 20 substrate	M7/Alloy20	Cr_2O_3/Ta/ Alloy20
OCP (V)	- 0.25	0.60	-019	-0.20	0.13	-0.06
E_{corr} (mV)	-247.82	460	-325.42	-191.30	-3.50	-141.83
i_{corr} ($\mu A/cm^2$)	8.08×10^3	3.92×10^{-3}	5.88	4.58	0.053	10.09

Corrosion Testing in Autoclave Slurry Solution at Elevated Temperatures

Figure 14 and 15 provide photographs of M7 coating on TiGr.2 and commercial Cr_2O_3 coating on TiGr.12 test samples in autoclave sulfuric acid slurry solution with a pH of 0.09. The exposure temperature and duration is 270°C (518 °F) and 90 days.

Figure 14 shows no surface degradation of the M7 coating after 90 days exposure, except that the TiGr.2 base metal is corroded in the area not protected by the M7 coating. However, Figure 15 does show a significant surface degradation for the commercial Cr_2O_3 coating after 90 days exposure indicating that corrosion may have happened to either the base metal or Cr_2O_3 coating; in either case the Cr_2O_3 offered no protection to the base metal.

Plotted weight changes of M7 and Cr_2O_3 coupons before and after 30, 60 and 90 day exposure tests are shown in Figure 16. The M7 sample suffered weight loss after 30 days of exposure and negligible weight loss between 30 to 90 days. Inspection after 30 days of exposure revealed that the initial weight loss is mainly due to the corrosion of TiGr.2 base metal but not the corrosion of M7 coating. Neither the M7 coating nor TiGr.2 base metal corroded further in the 30 to 90 day exposure test. However, the Cr_2O_3/TiGr.12 did not reach a steady state throughout the entire 90 day exposure test. Since TiGr.12 is considered more corrosion resistant than TiGr.2, we suspect that the Cr_2O_3 coating was more susceptible to corrosion rather than the TiGr.12 substrate. Further evidence of Cr_2O_3 coating corrosion is presented below in adhesion strength testing results and SEM analysis in Figure 17.

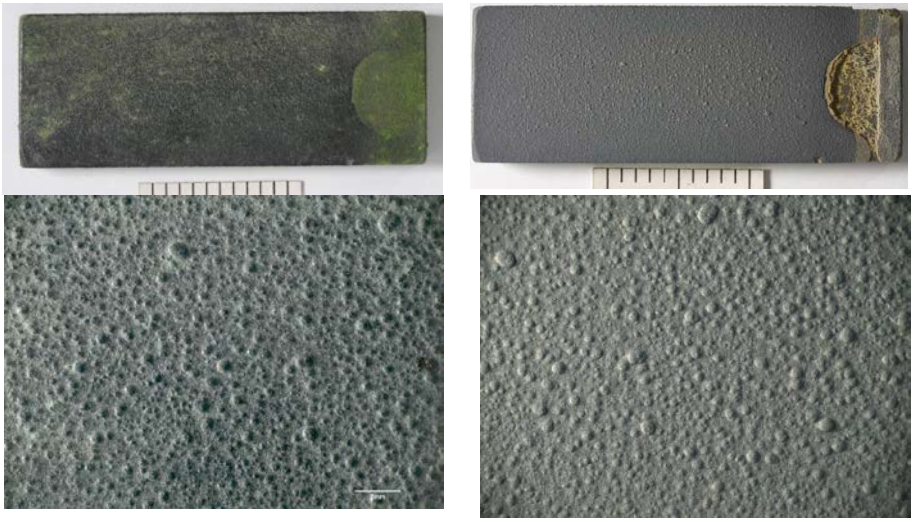

Before Exposure After 90 Day Exposure

Figure 14: Photographs of M7 coating on TiGr.2 coupons before (left) and after (right) 90 days exposure to 270 °C (518 °F) sulfuric acid solution of pH 0.09.

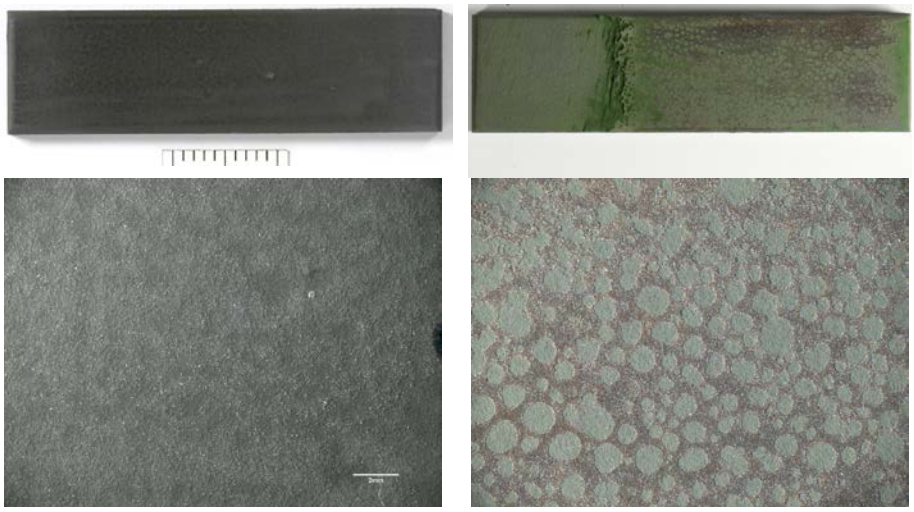

Before Exposure After 90 Day Exposure

Figure 15: Photographs of commercial Cr_2O_3 coating on TiGr.12 coupons before (left) and after (right) 90 days exposure to 270 °C (518 °F) sulfuric acid solution of pH 0.09.

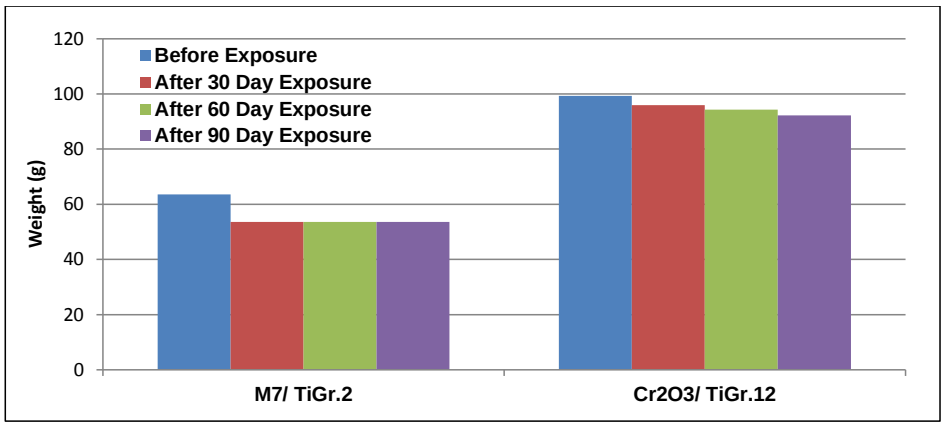

Figure 16: Weight changes of M7 coating on TiGr.2 and commercial Cr_2O_3 coating on TiGr.12 before and after 30, 60 and 90 day exposure to 270 °C (518 °F) sulfuric acid solution of pH 0.09.

Adhesion strength measurements for both M7 and Cr_2O_3 coating before and after 90 day exposure in autoclave slurry solution was performed. The adhesion strength of M7 has reduced 35% from 10,664 psi (before exposure) to 6,826 psi (after exposure). However, the adhesion strength of the Cr_2O_3 coating was reduced from 9,149psi (before exposure) to 0psi (after exposure); the Cr_2O_3 coating disintegrated when the surface was prepared for bond strength testing. The damaged surface is shown on the top right side in Figure 15 where 30% of the Cr_2O_3 coating delaminated during cleaning before bond strength testing.

SEM investigation of the cross section of the M7 coated TiGr.2 and the Cr_2O_3 coated TiGr.12 coupons after 90 day exposure further confirmed the damage to the Cr_2O_3. Figure 17 shows the cross section of the M7/TiGr.2 coupon with no sign of degradation of either the coating or the coating/base metal interface. However, the Cr_2O_3/TiGr.12 suffered severe degradation through the entire cross section down to the interface of the coating and TiGr.12 substrate. The Cr_2O_3 coating totally lost its integrity as the Cr_2O_3 was leached out of the coating which became porous.

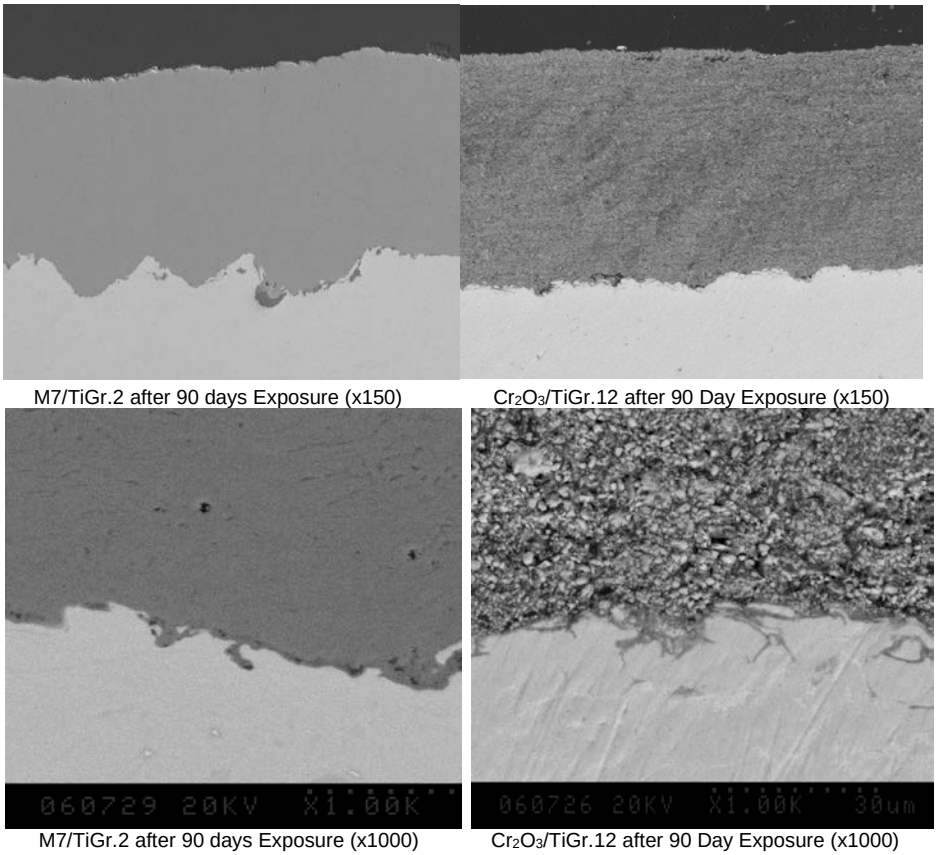

M7/TiGr.2 after 90 days Exposure (x150) | Cr_2O_3/TiGr.12 after 90 Day Exposure (x150)

M7/TiGr.2 after 90 days Exposure (x1000) | Cr_2O_3/TiGr.12 after 90 Day Exposure (x1000)

Figure 17: SEM photographs of M7/TiGr.2 and Cr_2O_3/TiGr.12 coupons after 90 days exposure to 270 °C (518 °F) sulfuric acid solution of pH 0.09.

Abrasion Resistance Evaluation

Over the past decade, several ball valve OEMs and their collaborators have published abrasion test results following the ASTM G65 standard. However, since the published results do not strictly follow the same procedure, it makes the comparison of the actual coating performance extremely difficult. Fortunately, the ASTM G65 standard specifies the load, wheel diameter and the number of revolutions for each procedure, therefore a trained tribologist can calculate abrasion resistance[16] in the unit of Nm/mm^3 by multiply the load (N) with the wheel diameter (m), with the total revolution and divide by the total volume loss (mm^3) for each sample.

The abrasion resistance of MOGAS samples and the samples published by other ball valve OEM's are calculated and presented in Figure 18.

The diamond symbols report wear resistance results from MOGAS samples X, Y, M7 tested using ASTM G65 procedure B, with material loss reported after 2000 cycles. The triangle symbols are the published samples[17] tested using a modified ASTM G65 procedure D with a lower applied load (45N vs. 130N used in other abrasion tests) but with 2000 revolutions instead of the 6000 revolutions called for by procedure D. The circular symbols are the published samples[18] tested using ASTM G65 procedure E, in this case material loss is reported after 1000 cycles (half of the number of cycles that MOGAS coatings were tested to).

Although the MOGAS adopted ASTM G65 procedure B has more severe test conditions than ASTM G65 procedure D and E, MOGAS M7 coatings still significantly out perform all other coatings in abrasion resistance. It is important to note that the higher hardness associated with Cr_2O_3 coating does not translate to higher abrasion resistance. The abrasion resistance evaluation results have further confirmed our previous findings that a combination of hardness and ductility for a ceramic coating is more advantageous than those coatings that only exhibit high hardness.

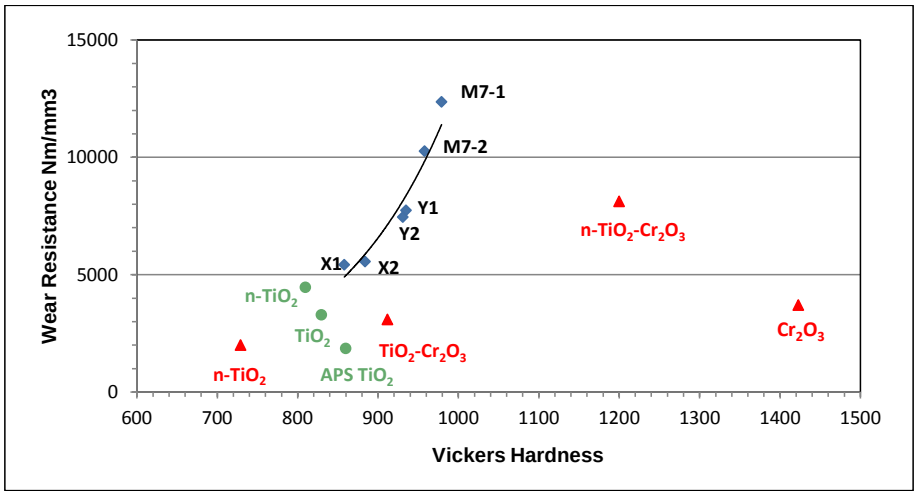

Figure 18: Abrasion resistance of sample X's, Y's and M7's and published similar coatings.

Field Performance

The photographs presented in Figure 19 compare the performance of our M7 coating and a conventional structured Cr_2O_3 coating from another valve manufacturer on 6" (150mm) Alloy 20 balls in oxygen supply service. The two valves had been installed in the same autoclave location and subjected to the same temperature, pressure and process media. Both valves were sent to MOGAS for service and coating evaluation after 6+ months in service. The photographs on the left are taken of the MOGAS ball with M7/F53 material. The photographs on the right are the other valve manufacturer's ball with Cr_2O_3/Ta/Alloy 20 material. After facing the identical service conditions, the MOGAS coating showed only minor surface scratching due to normal mechnical cycling. However, the coating supplied by the other valve manufacturer failed in service as a result of galvanic corrosion causing total coating loss and then erosion to the base metal. The only way coating materials could be identified on the other manufacturers valve was using X-ray diffraction methods from the coating residue found on the ball bore and on the seats.

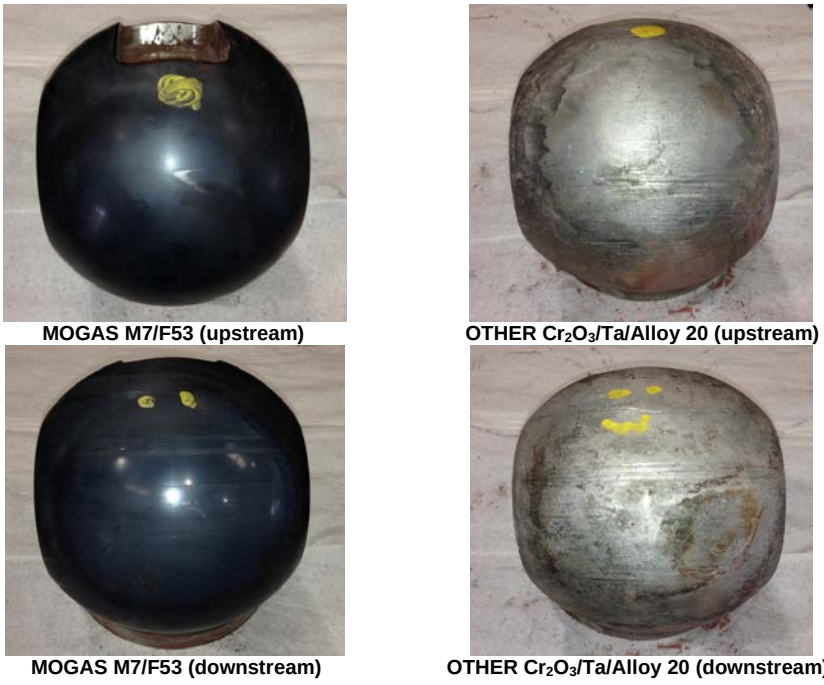

MOGAS M7/F53 (upstream) | OTHER Cr_2O_3/Ta/Alloy 20 (upstream)

MOGAS M7/F53 (downstream) | OTHER Cr_2O_3/Ta/Alloy 20 (downstream)

Figure 19: Photographs of field returned n-TiO_2 and Cr_2O_3 coated balls of 6" (150mm) autoclave isolation valves after more than 6 months service – M7/F53 (left) and Cr_2O_3/Ta/Alloy 20 (right).

Our standard practice is to continually analyze and test valves and coatings returned to our facilities for repair from the field. Within the past 12 months, bond strength tests were performed (before and after service) on 10" (250mm) Titanium Grade 12 valves (one coated with M7 coating and the other supplied with another valve manufacturers Cr_2O_3). Both valves were subjected to same service conditions and time in service.

Before and after service bond strength test results are presented in Table 5. Although both seats appeared to be in good condition before bond tests were performed, the bond strength of MOGAS M7 /Titanium Gr.12 was significantly higher than the other valve OEM's Cr_2O_3/Ta/Titanium Gr.12 seat which indeed had suffered significant bond strength loss while in service.

In fact it can be noted that the bond strength of the Cr_2O_3 coating had degraded over 50% faster than the n-TiO_2 coating when exposed to actual service conditions.

Table 5: Seats Coating Bond Strength Results Before and After Autoclave Service

Coating / Trim Material	Adhesion Strength (ASTM D4541) before service (coupons)	Adhesion Strength (ASTM D4541) after service (seats)
MOGAS M7/TiGr.12	10,443 psi	9,560 psi
Cr_2O_3/Ta/TiGr.12	> 7,000 psi	2,481 psi

SUMMARY

This study clearly demonstrates how significant coating properties can be improved through continued process improvement, additional production testing to identify possible coating weaknesses not identified by current production test methods and quality control protocol. This in return benefits coating and subsequently valve performance, increasing service life and reliability under extreme operating conditions.

MOGAS continues to work with our customers and end users to seek solutions to problems found in the autoclave industry and are committed to a program of continued research and development to improve our current coatings as well as develop the next breakthrough technology.

Some of the specific findings include:

1. M7 coating show the best physical and electrochemical properties; this new process is now in production at MOGAS coating facilities and will lead to improved performance and reliability of our valves over our current processes.

2. M7 coating combining higher hardness and toughness has demonstrated superior abrasion and corrosion resistance in both electrochemical and actual autoclave slurry testing compared with other commercial ceramic coatings when applied on industry accepted materials.

3. Both bend and low-load impact tests provide key information that will continue to be used to further differentiate the quality of M7 and other ceramic coatings, beyond commonly accepted coating specifications;

4. The Tafel polarization curves demonstrate a significant improvement in corrosion resistance of Titanium, Super Duplex and Superaustenitic stainless steels after the application of M7 coating.

5. M7 coating offers significant improvement to the corrosion resistance and toughness of F53 or Alloy 20 valves; this effect is more pronounced for F53 than Alloy 20 base materials.

6. Additional test methods, such as the ones presented here, will be critical in ensuring future advancements in coating performance and reliability for field applications.

REFERENCES

1. MIL-STD-1687A(SH), Department of the Navy, Naval Sea Systems Command, February 11, 1987.

2. J.A. Ellor, J. Repp, W.T. Young, Long Term Corrosion Control by Thermal Spray Metallic Coatings, 2003 Tri-Service Corrosion Conference.

3. Joint Standard, SSPC-CS 23.00/AWS C2.23M/NACE No. 12, Specification for the Application of Thermal Spray Coatings (Metallizing) of Aluminum, Zinc, and Their Alloys and Composites for the Corrosion Protection of Steel.

4. D. Wixson, Thermal Sprayed Deposits Shield Structures from Corrosion, Welding Journal, Vol. 88, Issue 7, January 2009, pp. 46-49.

5. Thermally Sprayed Metal Coatings to Protect Steel Pilings: Final Report and Guide, National Cooperative Highway Research Program, Report 528.

6. Hard Chrome Alternatives Team, Validation of HVOF Thermal Spray Coatings as Replacements for Hard Chrome Plating on Hydraulic/Pneumatic Actuators – Part I (Coupon Testing), August 2004.

7. D.J. Branagan, M. Breitsameter, B.E. Meacham, V. Belashchenko, High Performance Nanoscale Composite Coatings for Boiler Applications, Journal of Thermal Spray Technology, Volume 14, Issue 2, pp.196-204.

8. L. Moskowitz, K. Trelewicz, HVOF Coatings for Heavy-Wear, High-Impact Applications, Journal of Thermal Spray Technology, Volume 6, Issue 3, September 1997, pp. 294-299.

9. J.C. Farmer, Iron-Based Amorphous Metals: The High Performance Corrosion Resistant Materials(HPCRM) Program, Materials Science & Technology 2007 Conference and Exhibition, Detroit, MI, September 16-20, 2007.

10. M. Nakamichi, H. Kawamura, Mechanical and Electrical Properties of Al2O3-TiO2 Coating as Electrical Insulator, Thermal Spray 2001: New Surfaces for a New Millenium, Proceedings of the International Thermal Spray Conference, pp. 1039-1043.

11. B.D. Sartwell, K.O. Legg, J. Schell, J. Sauer, P. Natishan, D. Dull, J. Falkowski, P. Bretz, J. Devereaux, C. Edwards, D. Parker, Validation of HVOF WC/Co Thermal Spray Coatings as a Replacement for Hard Chrome Plating on Aircraft Landing Gear, Naval Research Laboratory, NRL/MR/6170—04-8762, March 31, 2004.

12. Williams J, Kim GE, Walker J. Ball Valves with Nanostructured Titanium Oxide Coatings for High-Pressure Acid-Leach Service: Development to Application. Proceedings of Pressure Hydrometallurgy 2004, Banff, Alberta, Canada, October 23-27, 2004.

13. Kim GE, Walker J. Successful Application of Nanostructured Titanium Dioxide Coating for High-Pressure Acid-Leach Application. Journal of Thermal Spray Technology, Volume 16(1), March 2007, p. 34.

14. Kim GE. Thermal Sprayed Nanostructured Coatings: Applications and Developments. Chapter 3 of Nanostructured Materials Processing, Properties, and Applications – 2nd Edition, Koch CC, editor. William Andrew Publishing, 2007.

15. Materials Testing – Mechanical Properties, Tensile Strength, Impact Strength, Hardness and Corrosion Resistance Handbook of Engineering Materials, Vol. 1. 5th Edition.

16. Yunfei Qiao, The effects of fuel chemistry and feedstock powder structure on the mechanical and tribological properties of HVOF thermal-sprayed WC–Co coatings with very fine structures, Surface and Coatings Technology 172 (2003) 24–41.

17. R.S. Lima*,From APS to HVOF spraying of conventional and nanostructured titania feedstock powders: a study on the enhancement of the mechanical properties, Surface & Coatings Technology 200 (2006) 3428– 3437

18. Luc Vernhes, Nanostructured and conventional Cr2o3, TiO2 and TiO2-Cr2O3 thermal sprayed coatings for metal seated ball valve applications in hydrometallurgy, ALTA 2013

19. J. Williams, G. E. Kim, J. Walker, Ball Valves with Nanostructured Titanium Oxide Coatings for High-Pressure Acid-Leach Service: Development to Application, ALTA 2004